Aging Cell (2012) **11,** pp986–995 Doi: 10.1111/j.1474-9726.2012.00869.x

Modelling *in vivo* skeletal muscle ageing *in vitro* using three-dimensional bioengineered constructs

Adam P. Sharples,[1,2] Darren J. Player,[1,2] Neil R. W. Martin,[1,2] Vivek Mudera,[4] Claire E. Stewart[3] and Mark P. Lewis[2,1,5,6]

[1]Muscle Cellular and Molecular Physiology Research Group (MCMPRG), Institute for Sport and Physical Activity Research (ISPAR Bedford), University of Bedfordshire, Bedford, UK
[2]Cellular and Molecular Physiology, Musculoskeletal Biology Research Group, School of Sport, Exercise and Health Science, Loughborough University, Loughborough, UK
[3]Faculty of Science and Engineering, Institute for Biomedical Research into Human Movement and Health (IRM), Manchester Metropolitan University, John Dalton Building, Oxford Road, Manchester, UK
[4]Institute of Orthopaedics and Musculoskeletal Sciences, UCL Division of Surgery & Interventional Science, Stanmore Campus, University College London (UCL), London, UK
[5]Cranfield Health, Cranfield University, Cranfield, Bedfordshire, UK
[6]School of Life and Medical Sciences, University College London (UCL), London, UK

Summary

Degeneration of skeletal muscle (SkM) with age (sarcopenia) is a major contributor to functional decline, morbidity and mortality. Methodological implications often make it difficult to embark on interventions in already frail and diseased elderly individuals. Using *in vitro* three-dimensional (3D) bioengineered skeletal muscle constructs that model aged phenotypes and incorporate a representative extracellular matrix (collagen), are under tension, and display morphological and transcript expression of mature skeletal muscle may more accurately characterize the SkM niche. Furthermore, an *in vitro* model would provide greater experimental manipulation with regard to gene, pharmacological and exercise (mechanical stretch/electrical stimulation) therapies and thus strategies for combating muscle wasting with age. The present study utilized multiple population-doubled (MPD) murine myoblasts compared with parental controls (CON), previously shown to have an aged phenotype in monolayer cultures (Sharples *et al.*, 2011), seeded into 3D type I collagen matrices under uniaxial tension. 3D bioengineered constructs incorporating MPD cells had reduced myotube size and diameter vs. CON constructs. MPD constructs were characterized by reduced peak force development over 24 h after cell seeding, reduced transcript expression of remodelling matrix metalloproteinases, MMP2 and MMP9, with reduced differentiation/hypertrophic potential shown by reduced IGF-I, IGF-IR, IGF-IEa, MGF mRNA. Increased IGFBP2 and myostatin in MPD vs. CON constructs also suggested impaired differentiation/reduced regenerative potential. Overall, 3D bioengineered skeletal muscle constructs represent an *in vitro* model of the *in vivo* cell niche with MPD constructs displaying similar characteristics to ageing/atrophied muscle *in vivo*, thus potentially providing a future test bed for therapeutic interventions to contest muscle degeneration with age.

Key words: satellite cell; MRF; IGF-I; IGFBP; myostatin; TNF.

Introduction

After the age of 50, humans lose skeletal muscle (SkM) mass at a rate of 1–2% per year (Hughes *et al.*, 2001). This phenomenon (sarcopenia) (Rosenberg, 1997) is a significant contributor to the loss of metabolic function (Russ & Lanza, 2011), physiological capacity and is strongly correlated with morbidity and mortality (Rantanen *et al.*, 2000). Sarcopenia is now recognized as a serious clinical disorder (Cruz-Jentoft *et al.*, 2010) in an attempt to summon adequate clinical management to address the problem in a rapidly expanding, ageing population. Adult skeletal muscle regeneration is largely dependent on a resident stem cell population of satellite cells (Mauro, 1961). Satellite cells are mononuclear cells that are peripherally located underneath the basal lamina of mature myofibres and can be activated upon relevant cues to proliferate. A subset of these satellite cells return to quiescence to renew the pool for future regenerative bouts, while the remainder progress into myoblasts, which migrate to the reparative site and differentiate/fuse to become incorporated into multinucleated myotubes, repairing the existing skeletal muscle fibre. This is fundamental in the way in which skeletal muscle displays its astounding plasticity during development, exercise, stretch and mechanical loading with an increase in size (hypertrophy). However, with such sensitive regulation, severe loss (atrophy) commonly occurs with ageing, disuse and disease that is characterized globally by changes in protein synthesis and protein degradation that lead to muscle mass reductions. Given the key roles that these cells play, it is imperative that they are critically investigated to provide better understanding of the processes underlying skeletal muscle ageing. This is particularly relevant, given recent findings, suggesting that human muscle-derived cells show impaired differentiation and thus reduced regenerative potential vs. the cells of younger donors (Pietrangelo *et al.*, 2009; Beccafico *et al.*, 2010), with an associated loss of myogenicity (Hidestrand *et al.*, 2008) yet without change in telomere length or telomerase activity (O'Connor *et al.*, 2009).

Myoblasts that have undergone multiple replicative divisions (Sharples *et al.*, 2010, 2011) or which display features of senescence *in vitro* (Bigot *et al.*, 2008) have been used to investigate ageing in monolayer cultures. Although these eloquent monolayer studies have modelled and thus revealed some important cellular and molecular mechanisms involved in the serial rounds of divisions with age and the regulation of senescence, owing to their single cell–layered nature, these models do not portray three-dimensional (3D) *in vivo* SkM structure [discussed in Sharples & Stewart (2011)]. Using a 3D bioengineered model of SkM that incorporates a representative extracellular matrix (type I collagen) is under tension and displays representative morphological, histological and transcript expression of mature skeletal muscle may more accurately characterize the SkM niche (Cheema *et al.*, 2003; Mudera *et al.*, 2010; Smith *et al.*, 2011). As a result, not only will these models act as a potential surrogate and reduce the need of often frail elderly *in vivo* human trials and biopsies, they will allow greater experimental manipulation, including gene knock-down, transfection, pharmacological interventions and the

Correspondence
Adam P. Sharples, Muscle Cellular and Molecular Physiology Research Group (MCMPRG), Institute for Sport and Physical Activity Research (ISPAR Bedford), University of Bedfordshire, Bedford, UK. Tel.: +4407812732670; e-mail: a.p.sharples@googlemail.com

Accepted for publication *31 July 2012*

ability to be 'exercised' *in vitro* (Player *et al.*, 2011). Further, a greater understanding of the cellular and molecular regulators of SkM during ageing will be available.

Therefore, in the present study, myoblasts were studied that had undergone multiple population doublings and thus potentially recapitulate the rounds of population expansion and self-renewal that occur *in vivo* across the lifespan (Sharples *et al.*, 2011). These myoblasts have previously been shown to display reduced regeneration in monolayer cultures, characterized by reduced morphological and biochemical differentiation, reduced cell cycle exit and associated decreases in IGF-I, myoD, myogenin mRNA and Akt signalling with increases in IGFBP5 mRNA and JNK signalling (Sharples *et al.*, 2011). Interestingly, similar morphology, transcript and signalling processes are also observed in cells isolated from elderly human muscle (Bigot *et al.*, 2008; Pietrangelo *et al.*, 2009; Beccafico *et al.*, 2010) and in whole tissue biopsies (Cuthbertson *et al.*, 2005; Leger *et al.*, 2008). Thus, by transferring these cells into 3D bioengineered type I collagen constructs this can potentially recapitulate, *in-vitro,* a model that represents aged skeletal muscle and displays a physiologically more relevant tissue, similar to that found *in-vivo,* allowing future manipulations in terms of therapeutic interventions in combating skeletal muscle wasting with age. Indeed, it is here reported that 3D bioengineered constructs incorporating myoblasts that have undergone multiple population doublings (MPD) have aligned but smaller and thinner myotube formation (atrophied) vs. aligned but thicker and larger myotubes (hypertrophied) in parental controls, shown by reductions in myotube size and diameter. These MPD constructs are characterized by reduced peak force development over 24 h after cell seeding, reduced transcript expression of remodelling matrix metalloproteinases (MMP2 and MMP9), with reduced differentiation/hypertrophic potential shown by reduced IGF-I, IGF-IR, IGF-IEa, MGF and increased IGFBP2 mRNA, and finally increased expression of catabolic transcripts (myostatin and TNF-α) vs. parental cellular constructs. Thus, providing an exciting future *in vitro* 3D bioengineered model that is more representative of an ageing/atrophied muscle *in vivo* in order to investigate the cellular and molecular mechanisms for deterioration of regeneration observed in skeletal muscle and provide a future test bed for pharmacological, gene and exercise therapies. Finally, this model could potentially be used for muscle-wasting disorders using diseased cells or for example in cachexia with the addition of influential systemic factors such as growth factors and cytokines such as tumour necrosis factor-alpha (TNF-α).

Materials and methods

Cell culture

C_2C_{12} murine skeletal myoblasts (Yaffe & Saxel, 1977; Blau *et al.*, 1985) (purchased from ATCC, Rockville, MD, USA) were grown in T75/T175 flasks in a humidified 5% CO_2 atmosphere at 37 °C in growth medium GM, composed of: Dulbecco's modified Eagle's medium/DMEM (Sigma, Poole, UK) plus 20% FBS (PAA Laboratories, Somerset, UK), and 1% penicillin–streptomycin solution (Invitrogen, Paisley, UK), until 80% confluence was attained. Prior to collagen/myoblast construct preparations, cells were washed twice in PBS, trypsinized and counted (1:1 trypan blue). 12×10^6 total cells were then pelleted via centrifugation at 2000 ***g*** for 5 min for use in specific experimentation.

Multiple population doublings of C_2C_{12} cells

Population doublings were carried out as in (Sharples *et al.*, 2011). Briefly, original stock C_2C_{12} mouse skeletal muscle cells were seeded at 1×10^6 cells in T75 flasks in 15 mL of GM and incubated for 48 h until ~80% confluent. Cells were trypsinized and seeded onto new T75s at 1×10^6 for 48 h or at 5×10^5 for 72 h, cell number and doubling time being recorded throughout. This cycle was repeated 20 times over 49 days, creating a stock of cells that had undergone 58 population doublings (multiple population doublings/MPD) (Sharples *et al.*, 2011) compared with the original stock that were retained in liquid nitrogen and had undergone no subsequent doublings (CON) relative to the MPD cells. These cells were used as the controls in all experiments reported here, that is, the same 'parental cells' that had produced their progeny were used as control cells. There was no observable cell death between cell expansions (determined by trypan blue).

Collagen/myoblast construct preparation

Constructs were prepared as previously published (Cheema *et al.*, 2003; Mudera *et al.*, 2010; Smith *et al.*, 2011). Supernatant was removed from the centrifuged 12×10^6 cell pellet and re-suspended in a volume of 0.1 mL GM. 2.6 mL of rat tail collagen type I (2.16 g mL^{-1}; First Link, Birmingham, UK) was added to 0.3 mL of 10× Eagle's Minimum Essential Medium (EMEM) (Gibco, Paisley, UK). The solution was neutralized in a drop-wise manner using 5 and 1 M sodium hydroxide. Following neutralization, 12×10^6 cells were added to the collagen/EMEM solution. This collagen/cell solution was set in standard dimension chamber slides ($45 \times 20 \times 10$ mm) between two pre-sterilized polyethylene mesh flotation bars, attached to the chambers via stainless steel frames (A-Frames; Fig. 1A). These constructs polymerized for 30 min in a humidified 5% CO_2 atmosphere at 37 °C before being detached using a 21-G needle. Five millilitres of GM was added to the chambers with the flotation bars facilitating resistance against the chamber slide to generate the uniaxial tension (Fig. 1A). After cell attachment (24 h), the myoblast/collagen constructs were washed ×2 PBS followed by 5 mL low-serum differentiation media (DM), composed of DMEM plus 2% horse serum, 1% penicillin–streptomycin solution. C_2C_{12} myoblasts undergo spontaneous differentiation into myotubes on serum withdrawal, and do not require growth factor addition (Yaffe & Saxel, 1977; Blau *et al.*, 1985). Constructs were fixed for imunno-histological analysis and lysed for transcript expression at 3, 7 and 14 days time points. Constructs were attached to a Culture Force Monitor (CFM) to measure force and rate of force development every minute for 24 h following initial seeding.

Culture Force Monitor measurements

The CFM is a custom built device that measures real-time force contraction of 3D cellular constructs (Eastwood *et al.*, 1994; Mudera *et al.*, 2010). This measurement was used to assess the amount of force developed by the cells attaching to the matrix over the first 24 h after seeding, as previously described (Cheema *et al.*, 2003; Mudera *et al.*, 2010), for both the MPD and CON cells seeded into type I collagen, as detailed previously. Amendments to the originally published system have been developed as part of this project (referred to as CFM mk2). The measuring beam of the CFM mk2 was manufactured from 0.15-mm Copper-Beryllium sheet (Goodfellow Metals Ltd, Cambridge, UK) cut into strips (100×10 mm). Transducer class strain gauges (Wellyn Strain Measurement, Basingstoke, Hants, UK) were attached to the Copper-Beryllium beams in a full bridge electrical network at 20 mm from one end. A hook was soldered onto the end of the measuring beam connected to the constructs through the stainless steel wire 'A frames' (Fig. 1A). The force transducer was attached through a wired mechanism to a Model P3 Strain Indicator and Recorder (Vishay, Basingstoke, UK) connected to a

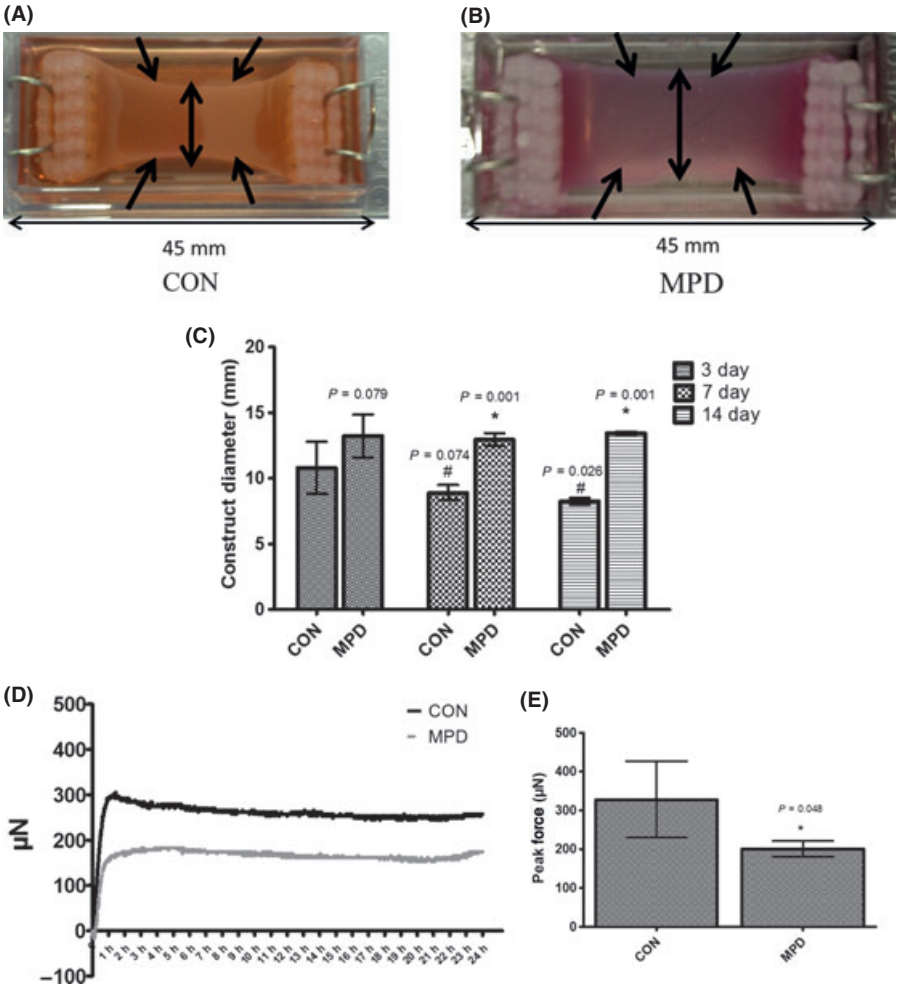

Fig. 1 (A,B) Depicts the control (CON; A) and multiple population doubling (MPD; B) collagen constructs that have been polymerised between the two flotation bars that are in-turn attached to the chamber slide via metal 'a-frames.' There was reduced bowing (indicated by →) and larger construct diameters (indicated by ↔) in MPD constructs vs. CON. (C) Depicts statistically significant reductions in construct diameter over the time course in CON cells but not MPD (#P = 0.001; C) and significantly impaired bowing in the MPD cells indicated by larger construct diameters in MPD cells at 3, 7 and 14 days (*P = 0.001; C). (D) Depicts the mean force traces of CON (black) vs. MPD (dark grey) after initial seeding into collagen matrices up to 24 h. (E) Depicts the statistically significant *difference in peak force that was impaired in MPD cells vs. CON.

computer via USB. This unit acted as a bridge amplifier, static strain indicator and digital data logger. Micro-strain (με) and time data were collected at a rate of 1 Hz (one reading per second) for all measurements. Before experimentation the force transducers were calibrated to provide an equation to convert the micro-strain (με) reading to micro-Newton's (μN). Force transducers were left in a humidified 5% CO_2 atmosphere at 37 °C for a period of 24 h and calibrated against known masses of 0.03, 0.05, 0.2, 0.3, 0.5 g, corresponding to 294, 491, 1962, 2943, 4905 μN (where: weight (g) was converted to Kg and multiplied by 9.81 m s^{-1} to calculate Newtons (N); the resultant was divided by 1000 to calculate μN). The micro strain (με) was recorded for each weight for 5 min and plotted against μN. The resultant linear equation was used to convert με to μN generated by the myoblast/collagen constructs. The με was recorded every minute for a period of 24 h after seeding the myoblasts in the collagen gels.

Immunohistology and microscopy

Whole mounted constructs were washed ×2 with PBS and fixed (3.7% paraformaldehyde), permeabilized, blocked (0.2% Triton, 2% Goat Serum, diluted in TBS solution) and stained using mouse monoclonal anti-desmin antibody (diluted 1 in 200; Sigma). Secondary antibody, goat anti-rabbit IgG TRITC (diluted 1:200; Sigma) was added to enable fluorescent detection. SYTOX® nuclear stain (Molecular Probes, Paisley, UK) diluted 1 in 2000 was used to counterstain nuclei. The sections were visualized using a Zeiss LSM 510 fluorescent microscope (40×) with manufacturer's software. TRITC was excited at 485 nm and emitted at 520 nm and appears red in images presented. SYTOX® nuclear stain was excited at 504 nm and emitted at 523 nm and appears green. Images for all conditions were taken and analysed for morphological analyses of myotube area (μm^2) and diameter (μm) using IMAGE J (Java) software (National Institute of Health, Bethesda, MD, USA).

RNA extraction and analysis

Constructs were immersed and homogenized in 0.5 mL TRIzol. RNA was extracted according to manufacturer's instructions. RNA concentration and purity were assessed by UV spectroscopy at ODs of 260 and 280 nm using a Nanodrop 3000 (Fisher, Rosklide, Denmark). 70 ng RNA was used for each PCR reaction.

Primer design

Primer sequences (Table 1) were identified using Gene (NCBI, http://www.ncbi.nlm.nih.gov/gene) and designed using both web-based Oligo-Perfect™ Designer (Invitrogen, Carlsbad, CA, USA) and Primer-BLAST (NCBI, http://www.ncbi.nlm.nih.gov/tools/primer-blast). Sequence homology searches ensured specificity. The primers were ideally designed

to yield products spanning exon-exon boundaries to prevent any amplification of gDNA. Three or more GC bases in the last five bases at the 3′ end of the primer were avoided. Secondary structure interactions (hairpins, self-dimer and cross dimer) within the primer were avoided. All primers were between 18 and 23 bp, and amplified a product of between 76 and 350 bp. GC content was between 38.1% and 55.6% (Table 1). Primers were purchased from Sigma (Suffolk, UK) without the requirement of further purification.

Reverse transcriptase quantitative Real-Time Polymerase Chain Reaction (rt-qRT-PCR)

rt-qRT-PCR amplifications were performed using QuantiFast™ SYBR® Green RT-PCR one step kit on a Rotogene 3000Q (Qiagen, Crawley, UK) supported by rotogene software (Hercules, CA, USA). rt-qRT-PCR was performed as follows: Hold 50 °C for 10 min (reverse transcription/cDNA synthesis), 95 °C for 5 min (transcriptase inactivation and initial denaturation step) and PCR Steps of 40 cycles; 95 °C for 10 s (denaturation), 60 °C for 30 s (annealing and extension). Upon completion, dissociation/melting curve analyses were performed to reveal and exclude non-specific amplification or primer-dimer issues. The relative gene expression levels were calculated using the comparative C_t ($^{\Delta\Delta}C_t$) equation otherwise known as the Livak method (Schmittgen & Livak, 2008), where the relative expression is calculated as $2^{-\Delta\Delta C_t}$ and where C_t represents the threshold cycle. Following screening of GAPDH, RPII-α and RPII-β; RPII-β showed the most stable C_t values and was selected as the reference gene in all RT-PCR assays. A pooled C_t value (17.4 ± 1.02) for the housekeeping gene, RPII-β, was derived from all rt-qRT-PCR runs. To compare MPD C_2C_{12} cells with CON C_2C_{12}, proliferating monolayer CON cells that had been grown in GM for 24 h and then transferred to DM for 30 min (0 h time point) were routinely used as the calibrator condition in the Ct ($\Delta\Delta C_t$) equation. Rt-qRT-PCR data presented in results/figure are therefore relative gene expression levels determined by the $\Delta\Delta C_t$ equation.

Table 1 Real time qPCR primer sequences

Target gene	Primer Sequence (5′–3′)	Ref. seq. number	Amplicon length (bp)
IGF-I	F: GCTTGCTCACCTTTACCAGC R: TTGGGCATGTCAGTGTGG	NM_010512	280
IGF-IR	F: TGCGGTGTCCAATAACTAC R: TGTTGATGGTGGTCTTCTC	NM_010513.2	110
IGF-IEa	F: GCTTGCTCACCTTTACCAGC R: AATGTACTTCCTTCTGGGTCT	NM_010512	300
IGF-IEb/MGF in mouse	F: GCTTGCTCACCTTTACCAGC R: AAATGTACTTCCTTTCCTCTC	NM_010512	353
IGFBP5	F: GAAGAGGTGGTGACAGAG R: TGACAACAAGATCGGGAA	NM_010518.2	104
IGFBP2	F: AGTGCCATCTCTTCTACAA R: GCTCAGTGTTGGTCTCTT	NM_008342.3	197
Myogenin	F: CCAACTGAGATTGTCTGTC R: GGTGTTAGCCTTATGTGAAT	NM_031189.2	173
Myostatin	F: TACTCCAGAATAGAAGCCATAA R: GTAGCGTGATAATCGTCATC	NM_010834.2	194
TNF-α	F: TCAACAACTACTCAGAAACAC R: AGAACTCAGGAATGGACAT	NM_013693.2	130
TNFRI	F: CTGATCTCTATCTGCCTCTG R: CGCTCGTGAATGAAGTAAG	NM_011609.4	101
MMP2	F: GACAAGTTCTGGAGATAC R: TAATAAGCACCCTTGAAG	NM_008610.2	155
MMP9	F: CTGGCAGAGGCATACTTG R: GCCGTAGAGACTGCTTCT	NM_013599.2	76
RP-IIB	F:GGTCAGAAGGGAACTTGTGGTAT R:GCATCATTAAATGGAGTAGCGTC	NM_153798.2	197

Statistical analyses

Statistical analyses were determined using MINITAB version 16.0 (Minitab Inc., PA, USA and LEAD Technologies, Inc., NC, USA). Results are presented as mean ± standard deviation (SD). Statistical significance for interactions between cell type (CON and MPD) and time (3, 7 and 14 days) were determined using (2 × 3) mixed two-way Factorial ANOVA. Results for factorial ANOVA's Post hoc analyses (with Bonferroni correction) were conducted where main effects for cell type or time occurred, without a significant interaction between time and cell type. If there were significant interactions present, independent *t*-tests were conducted to confirm statistical significance between variable of interest e.g. between cell types, and paired-sample *t*-tests undertaken for variable of interest within cell type and time. For all statistical analyses, significance was accepted at $P \leq 0.05$.

Results

Maintained construct diameter and lower force in multiple population doubling (MPD) bioengineered constructs vs. controls

Myoblasts, once seeded within the constructs, to mature, must first attach to the matrix and remodel this matrix (also see MMP expression below) to differentiate and fuse into myotubes at later time points (Mudera *et al.*, 2010). This attachment, then subsequent fusion creates a characteristic bowing morphology in the constructs (Fig. 1A; indicated by →). The changes in bowing can be grossly measured via construct diameter (mm; indicated as ↔ in Fig. 1A). Morphologically, MPD cells maintained construct diameter at all time points (Fig. 1B) vs. CON cells (Fig. 1A) where construct diameter reduced across the time course (3 days; 13.22 ± 1.64 mm, MPD vs. 10.8 ± 1.98 mm, CON, $P = 0.079$, 7 days; 12.9 ± 0.49 mm, MPD vs. 8.9 ± 0.58 mm, CON, $P \leq 0.001$, 14 days; 13.43 ± 0.13 mm, MPD vs. 8.24 ± 0.27 mm, CON, $P \leq 0.001$; Fig. 1C). This was suggestive that the CON cells were attaching to the matrix whereas MPD cells may have displayed an inability to attach to the matrix suggested previously (Cheema *et al.*, 2003; Mudera *et al.*, 2010). Indeed, this also resulted in a smaller average force trace (Fig. 1D) and reduced peak force in MPD cells vs. CON over the initial 24 h (Fig. 1E) after seeding within the collagen matrices (CON, 327.38 ± 98.87 vs. MPD, 200.79 ± 20 μN; $P = 0.048$, Figs 1D,E).

MPD cells have reduced matrix remodelling potential vs. control CON cells

In addition to reduced force generating potential and bowing, indicative of reduced cell attachment (Cheema *et al.*, 2003; Mudera *et al.*, 2010), MPD cells in type I collagen matrices also show average reductions in expression of matrix metalloproteinase 2 at both 3 and 7 days (3 days; 7.29 ± 1.74, MPD vs. 12.32 ± 3.72, CON, $P = 0.071$, 7 days; 15.08 ± 2.74, MPD vs. 27.79 ± 11.49, CON, P = NS; Fig. 2A), by 14 days MMP2 transcript expression was similar between MPD and CON (Fig. 2A). Significant and similar trends were observed in MMP9 expression at 3 days (Fig. 2B), where MPD cells had impaired expression vs. CON (3 days; 0.98 ± 0.14, MPD vs. 1.68 ± 0.32, CON, $P = 0.016$; Fig. 2B). Although expression remained impaired in MPD vs. CON cells at 7 and 14 days, the

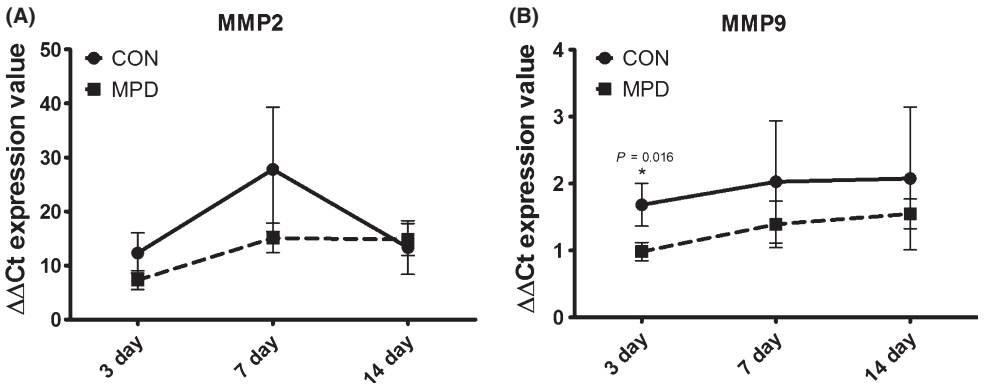

Fig. 2 Average reductions in expression of matrix metalloproteinase 2 (MMP2) mRNA specifically at early time points 3 and 7 days was non-significant (A), however, MMP9 was significantly lower in MPD myoblasts at 3 days indicated by * (B). Data is taken from three experiments in duplicate.

differences were non-significant (Fig. 2B). Overall, trends suggest early mean reductions in MMP2 and significant early decreases in MMP9 may underpin the impaired ability to degrade the matrix to initiate both cell matrix (indicated via reduced bowing and inability to contract the matrix in MPD cells; described above) and cell-cell interactions; a perquisite for myoblast differentiation/fusion into myotubes, a phenotype that is also impaired in the MPD cells (Sharples *et al.*, 2011). Immuno-staining for desmin in the constructs illustrates impaired myoblast fusion in MPD constructs, manifested by smaller, thinner myotubes vs. extensive and larger myotubes in CON constructs (Fig. 3A vs. Fig. 3B).

Reduced myotube size and diameter is observed in MPD constructs vs. control

Both constructs were aligned morphologically like skeletal muscle *in vivo* (Fig. 3C,D, and; after quantification of myotube size and area at 14 days MPD constructs showed significantly smaller and thinner myotubes vs. CON constructs (size μm^2: 2696 ± 334 in MPD vs. 4976 ± 928 in CON; $P = 0.05$, Fig. 3C; and diameter, μm: 15.38 ± 1.53 in MPD vs. 30.16 ± 4.79 in CON; $P = 0.036$, Fig. 3D). Overall indicating an atrophied skeletal muscle constructs using MPD cells vs. hypertrophied constructs (CON).

Reduced differentiation/hypertrophy in 3D bioengineered myoblast/collagen constructs in MPD cells vs. CON is underpinned by reductions in transcript expression of myogenic regulatory factor; myogenin, and insulin-like-growth factor family members: IGF-I, IGF-IR, IGF-IEa and MGF

Decreased transcript expression of the differentiation regulator, myogenin further substantiated the morphological analyses. Expression was

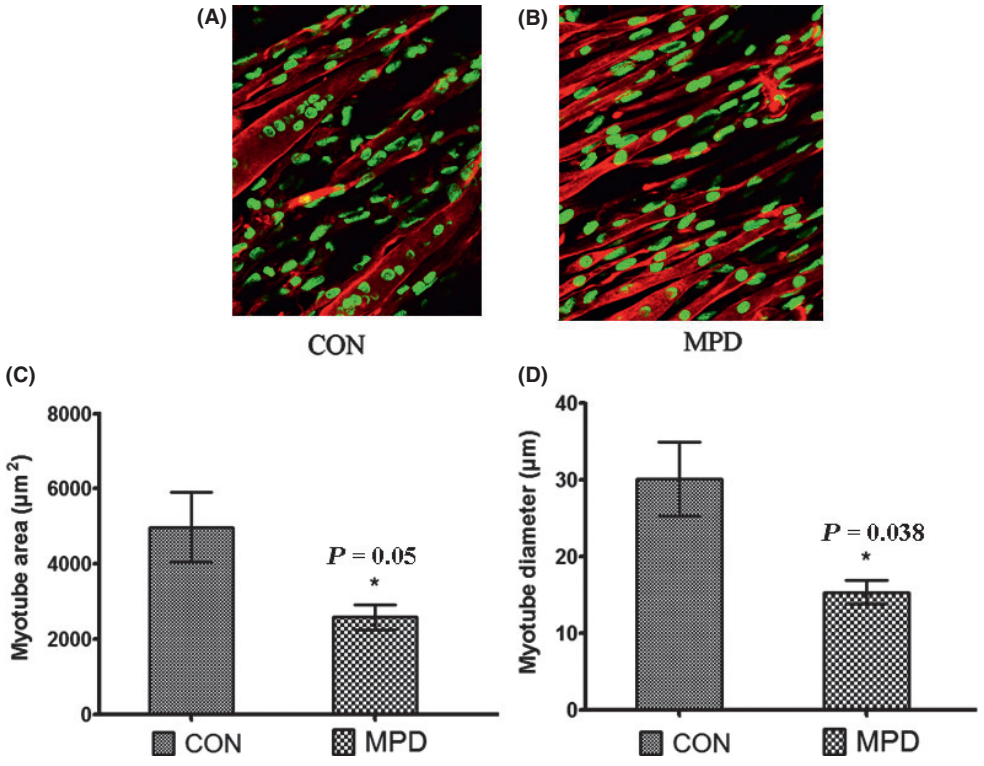

Fig. 3 (A) CON vs. (B) MPD collagen constructs differentiated over a 14 day period both demonstrating aligned myotube structures. CON constructs show larger and thicker myotube structures (hypertrophied) vs. MPD constructs that have smaller and thinner constructs (atrophied). (C) Myotube area and (D) myotube diameter morphological analyses also suggested that there was a statistically significant reduction in myotube area ($P = 0.05$) and diameter ($P = 0.038$) in MPD constructs. Confirming the atrophied phenotypes in MPD constructs vs. control constructs.

reduced at all times points, approaching significance at 3 days and reaching significance at 7 days (3 days; 2.5 ± 0.39, MPD vs. 6.19 ± 2.94, CON, $P = 0.089$, 7 days; 3.49 ± 0.54, MPD vs. 7.04 ± 1.76 mm, CON, $P \leq 0.031$, 14 days; 4.89 ± 1.3, MPD vs. 6.5 ± 1.93, CON, P = NS; Fig. 4A). Expression of IGF-I and its receptor, IGF-IR, were significantly decreased at 3 days in MPD vs. CON cells (IGF-I 3 days; 0.44 ± 0.21, MPD vs. 1.99 ± 0.6, CON, $P = 0.016$, Fig. 4B, IGF-IR 3 days; 0.46 ± 0.05, MPD vs. 0.82 ± 0.03, CON, $P = 0.001$; Fig. 4C), however, despite reductions continuing over the 14 days period, significance was not attained for IGF-I. IGF-IR was also not significantly different between MPD and CON at 7 days (Fig. 4C). Interestingly, however, IGF-IR expression was significantly greater at 14 days in MPD constructs vs. CON (0.69 ± 0.04 MPD vs. 0.56 ± 0.02, CON, $P = 0.003$; Fig. 4C), perhaps indicating a delayed temporal response. IGF-IEa was decreased early in MPD constructs relative to CON, as was MGF (IGF-IEa 3 days; 0.57 ± 0.31, MPD vs. 1.82 ± 0.59, CON, $P = 0.02$, Fig. 4D, MGF 3 days; 0.41 ± 0.28, MPD vs. 0.89 ± 0.13, CON, $P = 0.036$; Fig. 4E). MGF constructs at 7 days had reduced levels at this time point, that almost achieved significance (7 days; 0.43 ± 0.29, MPD vs. 0.87 ± 0.12, CON, $P = 0.064$; Fig. 4E). At 14 days there were no significant differences observed between MPD constructs for IGF-IEa or MGF (Fig. 4D,E).

IGFBP2 remains high across the 14 day time course in MPD constructs vs. a high to low temporal expression in CON, in the face of unaltered IGFBP5

It has previously been shown that for adequate differentiation of myoblasts to occur, IGFBP2 expression must decrease across the time course (Ernst *et al.*, 1992; Sharples *et al.*, 2010). Therefore, the high levels observed across the time course in MPD constructs vs. the high to low temporal expression in CON constructs may contribute to the reduced differentiation potential observed. At 3 days levels are high and comparable in both MPD and CON constructs (3 days; 0.12 ± 0.07, MPD vs. 0.07 ± 0.04, CON, P = NS; Fig. 4F), however, maintained high levels were observed in MPD cell at 7 (significant) and 14 days (approaching significance) vs. a reduction in CON cells across the time course (7 days;

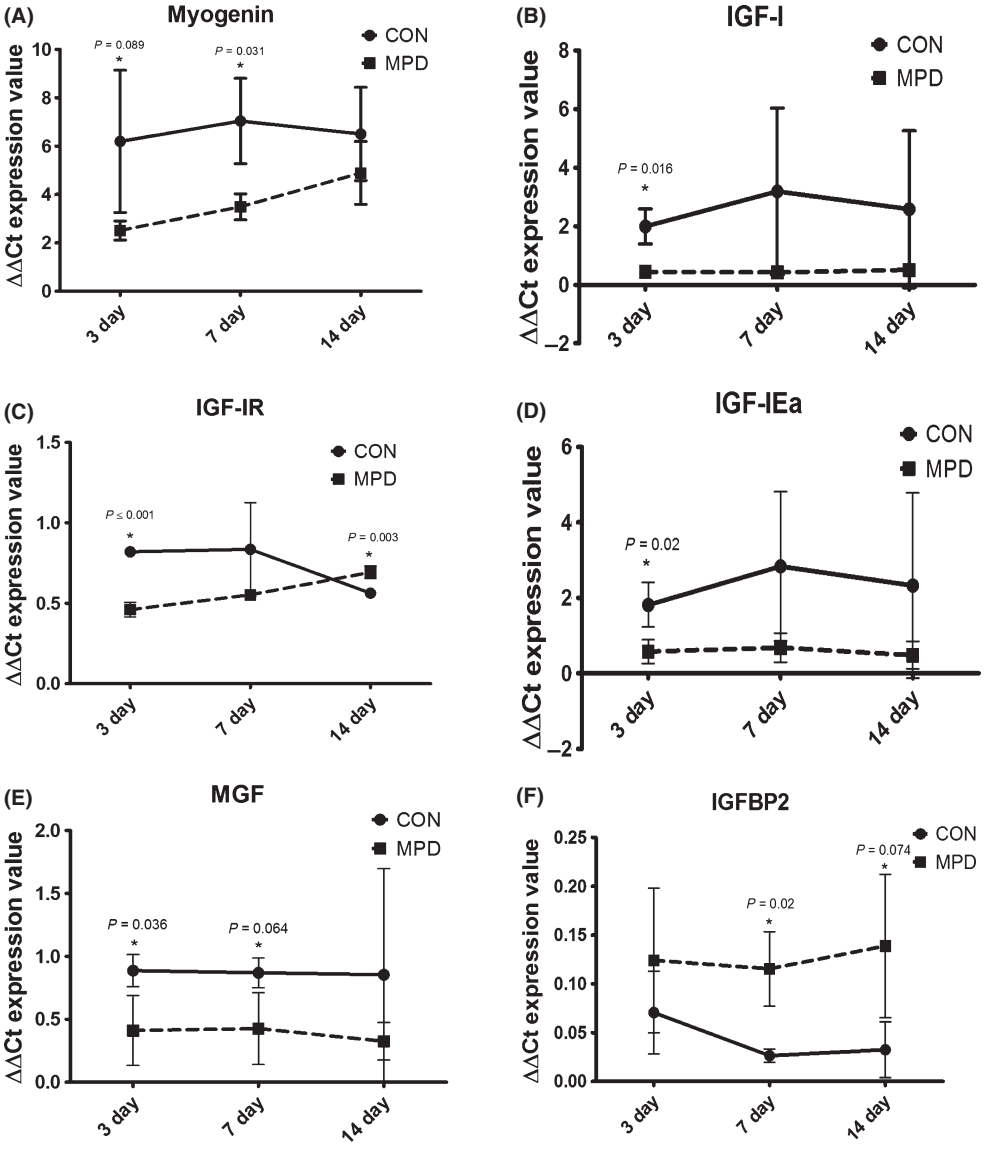

Fig. 4 (A) Myogenin mRNA is reduced at all times points, reaching significance at 7 days. (B) Insulinlike-growth factor-I (IGF-I) and its receptor, IGF-IR (C) are significantly decreased at 3 days in MPD constructs. IGF-IR expression was significantly greater at 14 days in MPD constructs vs. CON (indicated by *, C), perhaps indicating a delayed temporal response. (D) IGF-IEa was decreased early (3 days) in MPD constructs relative to CON, as was MGF (E). MGF approached significance with reduced expression at 7 days (E). (F) IGFBP2 levels are high in both MPD and CON constructs shown by similar expression, however MPD cells maintained high levels at 7 (significant) and 14 days (approaching significance) vs. a reduction in CON cells across the time course. Data is taken from three experiments in duplicate.

0.11 ± 0.04, MPD vs. 0.03 ± 0.01, CON, $P = 0.02$, 14 days; 0.14 ± 0.07, MPD vs. 0.03 ± 0.03, CON, $P = 0.074$; Fig. 4F). Despite expression levels of IGFBP5 being increased in MPD vs. CON constructs at 7 and 14 days, significance was not attained (data not shown).

Increased myostatin and TNF-α but not TNFRI further underpin differences between MPD and CON constructs

Myostatin expression is not significantly different between CON and MPD constructs at early time points (3 days; 107.97 ± 39.69, MPD vs. 283.14 ± 220.98, CON, P = NS; Fig. 5A) and late time points (14 days; 162 ± 56.86, MPD vs. 142.03 ± 85.46, CON, P = NS; Fig. 5A), however, is significantly increased in MPD constructs vs. CON at 7 days (128.33 ± 16.38, MPD vs. 80.92 ± 19.83, CON, $P = 0.014$, Fig. 5A). TNF-α was also increased in MPD cells at the 7 days time point vs. CON constructs (29.16 ± 8.94, MPD vs. 13.07 ± 4.02, CON, $P = 0.014$; Fig. 5B), again without (like myostatin) significant differences at early and late time points (3 days; 24.15 ± 15.68, MPD vs. 41.9 ± 41.45, CON, P = NS, 14 days; 41.8 ± 29.57, MPD vs. 27.8 ± 4.2, CON, P = NS; Fig. 5B). Despite a significant difference in TNF-α, its associated receptor TNFRI was unchanged at any time point (data not shown).

Discussion

The present study utilized a current murine myoblast replicative ageing model (Sharples *et al.*, 2011), a concept that has been used to investigate senescence in human myoblasts (Mouly *et al.*, 2005; Bigot *et al.*, 2008), to develop novel three-dimensional (3D) bioengineered skeletal muscle constructs that displayed reduced differentiation and atrophied morphology vs. their parental, non-divided controls. Firstly, this model provided a more physiologically relevant tissue with respect to *in vivo* muscle fibres, as can be seen by the aligned myotubes (Fig. 3A,B) vs. that of monolayer cultures that display swirling myotubes owing to lack of unilateral tension. Secondly, using this model, myotubes are smaller/thinner in the MPD constructs vs. parental controls; a phenotype of ageing skeletal muscle fibres measured histologically (Edstrom & Ulfhake, 2005), in cells that have been isolated and induced to differentiate (Pietrangelo *et al.*, 2009; Beccafico *et al.*, 2010) and finally at the *in vivo* level indicated via reductions in physiological cross sectional area (Morse *et al.*, 2005a). Indeed, it should be noted that type I collagen used to generate the 3D dimensional constructs in the present study, is only one extracellular matrix molecule that is not necessarily representative of complex *in-situ* muscle ECM. However, perimysial collagen is predominantly type I, whereas type III collagen appears to be more evenly distributed between endomysium and epimysium (Gillies & Lieber, 2011). Future work may wish to incorporate type III collagen into these constructs to further mimic the cell niche. However, the present model certainly supersedes monolayer models of ageing myoblasts with respect to morphology that is representative of skeletal muscle *in-vivo*.

In addition to the smaller, thinner myotubes observed in MPD constructs they also displayed significant decreases in myogenin mRNA, a muscle specific transcription factor that is directly involved in fusion by promoting the expression of key cytoskeletal transcripts and proteins such as; myosin heavy chains, troponin, creatine kinase, titin and desmin in order for regeneration to occur [reviewed in Berkes & Tapscott (2005)]. Indeed, a reduction in myogenin and thus differentiation has been previously observed in replicatively aged human and mouse myoblasts (Bigot *et al.*, 2008; Sharples *et al.*, 2011). Despite this, a recent investigation suggested that myoD and myogenin levels were increased with age, and proposed as mechanism/drive in an attempt to attempt to compensate for the reduction in muscle mass with age (Edstrom & Ulfhake, 2005). However, the changes in myoD/myogenin in these *in vivo* studies should be viewed with caution, since mRNA isolated from whole muscle contains a mixture of mature fibres and satellite cells/myoblasts. MyoD/myogenin are still expressed in mature fibres to maintain transcriptional control and cytoskeletal integrity (Ferri *et al.*, 2009) as well as highly expressed in regenerating myoblasts. Levels could therefore be under/overestimated if regenerative processes are altered in ageing. It is therefore possible that the mature fibres are producing myoD/myogenin to a greater extent than the activated satellite cells in elderly individuals, with investigations suggesting that muscle cells isolated from elderly populations show reduced myoD/myogenin once isolated in culture (Bigot *et al.*, 2008). This indeed seems to be the case in the present study, where myogenin is reduced significantly in MPD vs. CON at 3 and 7 days while the constructs are continuing to differentiate, whereas at 14 days when the constructs are differentiated, myogenin is not significantly different to CON constructs.

Insulin-like growth factors (IGFs) influence hypertrophy of primary and cell line skeketal muscle cultures; enhancing proliferation, differentiation (Florini *et al.*, 1996), survival (Stewart & Rotwein, 1996), satellite cell recruitment (Jacquemin *et al.*, 2004) and myofibrillar protein accretion (Quinn *et al.*, 2007). Local IGF-I production by skeletal muscle is also important in hypertrophy, where liver deficient IGF-I mice showed similar strength gains vs. controls following overload via increases in IGF-I receptor tyrosine phosphorylation. Therefore, as IGF-I has been shown to be reduced in both the circulation (Benbassat *et al.*, 1997) and locally by the muscle in elderly individuals (Welle *et al.*, 2002; Leger *et al.*, 2008) and has the ability to restore skeletal muscle mass in old mice (Barton-Davis *et al.*, 1998), the reduction in IGF-I by the MPD constructs seems to mimic this reduced response. This reduction in IGF-I certainly seems to underpin

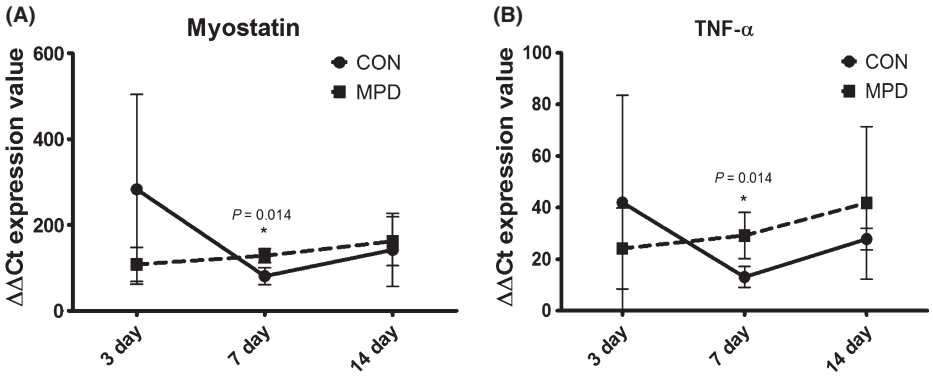

Fig. 5 (A,B) Myostatin (A) and TNF-α (B) mRNA are significantly increased in MPD constructs vs. CON at 7 days. Data is taken from three experiments in duplicate.

the inability of the cells to differentiate, as described previously in monolayer cultures with corresponding decreases in downstream Akt (Sharples *et al.*, 2011). It is however worth pointing out that at 7 and 14 days in the present study, although there was mean reductions in IGF-I, this was not significant. This would oppose the *in vivo* findings of reduced mRNA levels in elderly muscle tissue taken from biopsies. Recent evidence has however, begun to question the role of IGF-I in hypertrophy of mature skeletal muscle, especially following damage, with the inhibition of IGF-I signalling (mice overexpressing a dominant negative form of IGF-IR or 'MKR' mice), eliciting similar hypertrophic responses, following synergistic ablation of the plantaris muscle compared to wild-type mice (Spangenburg *et al.*, 2008); suggesting IGF is not important in hypertrophy following overload. Recently, the mechanisms for this have become clear where mechanical stimulation can directly activate signals downstream yet independently of IGF-I/Akt signalling (Miyazaki *et al.*, 2011), with mammalian target of rapamycin mTOR a key regulator of this hypertrophic response (Miyazaki *et al.*, 2011). The evidence for the role of IGF-I in myoblast differentiation and thus regeneration for homoeostasis rather than after overload, however, is fairly robust (Coolican *et al.*, 1997; Al-Shanti & Stewart, 2008), and indeed, even when using the MKR mouse model, it was shown that IGF-I is fundamental in myoblast fusion, with primary MKR myoblasts showing impaired differentiation, vs. wild-type controls, following damage (Heron-Milhavet *et al.*, 2010). Therefore, it is feasible that the reduction of IGF-I, as observed in the present MPD model, may account for the overall reductions in transcript found in muscle biopsies taken from older individuals, rather than the basal production from mature fibres. Overall, implicating the mitotically capable satellite cell further in its effect on the degenerative phenotype observed in skeletal muscle with respect to IGF-I production.

It has also been established that a significant relationship between lower resting levels of MGF (an isoform of IGF-I; IGF-IEc in humans/IGF-IEb in mice) and lower whole muscle cross sectional area in elderly people (Hameed *et al.*, 2004). Furthermore, elderly individuals have blunted responses to mechanical stimulation with respect to these isoforms (Owino *et al.*, 2001). Indeed, both of these isoforms were reduced in the present model. *In-vitro*, it has been demonstrated knock-down of IGF-IEa in C_2C_{12} cells causes differentiation and subsequent hypertrophy of myotubes but the inhibition of proliferation, whereas MGF has the opposite effect (activation of proliferation/inhibition of differentiation) (Yang & Goldspink, 2002). It is therefore not surprising that following resistance exercise, MGF is expressed temporally before IGF-IEa as this would mean proliferation predominates initially after damage followed by differentiation for repair (Owino *et al.*, 2001; Yang & Goldspink, 2002; Hameed *et al.*, 2003). Owino *et al.* (2001) showed that overload increased MGF expression in both young and old individuals; however, the expression reached a plateau at 24 h in elderly vs. a continued increase over 5 days in young. As these transcripts are reduced in the current MPD model this results in a similar response to base line/resting levels *in vivo* human studies, however, MGF is significantly lower in MPD cells at both 3 and 7 days, suggesting that the cells may reduce their proliferation and enhance differentiation vs. CON cells that have higher levels (Yang & Goldspink, 2002). However, this was not observed in monolayer, where MPD cells continue to cycle and not exit the cell cycle in G1 to differentiate (Sharples *et al.*, 2011) and also not observed phenotypically in the current 3D model. It is worth noting that lower MGF levels in MPD cells vs. CON is also in the face of reduced IGF-IEa that would impair differentiation. Further, it is noticeable that cells in these 3D construct do not differentiate as quickly (between 7 and 14 days – Fig. 3A) in both CON and MPD cells as in monolayer where myotubes begin forming after 48 h following serum withdrawal in monolayer (Sharples *et al.*, 2010, 2011). Therefore, together with reduced IGF-IEa levels the change in niche may account for the discrepancy in MGF levels across the time course of differentiation. This model warrants further investigation with respect to MGF and IGF-IEa responses following mechanical stimulation, and could provide an interesting model to elucidate delayed temporal responses to key anabolic mechanisms following exercise, as this model can be mechanically stretched *in vitro* (Cheema *et al.*, 2005; Player *et al.*, 2011).

IGF binding proteins (IGFBPs) modulate and mediate IGF-I action. Specifically, IGFBP2 binds IGF-I with high affinity and can manipulate its binding to the IGF-I receptor. It has previously been shown that IGFBP2 at high levels correlates with proliferation and reduces as cells differentiate (Ernst *et al.*, 1992; Sharples *et al.*, 2010). In the present study the MPD constructs have high expression at all-time points suggesting a mechanism for the reduced differentiation observed, where the CON group have a high to low expression across the investigated time course, which has previously been linked with enhanced differentiation (Sharples *et al.*, 2010). The mechanism by which IGFBP2 achieves this may be due to its direct role in binding to IGF-I and inhibiting the subsequent binding to the IGF-IR, or owing to an indirect mechanism whereby IGFBP2 has been shown to bind to the $\alpha5\beta1$ integrin receptor via the integrin arginine-glycine-aspartate (RGD) motif in its C terminal domain (Binkert *et al.*, 1989). This interaction, potentially alters Akt phosphorylation, downstream of the IGF-I receptor, following integrin-induced FAK phosphorylation and alteration in the phosphatase and tensin homologue, PTEN (Wheatcroft & Kearney, 2009). However, this mechanism is yet to be fully determined in skeletal muscle per se, and thus, no evidence for a role in ageing muscle is currently available. This therefore requires further investigation, especially as high expression across the time course is evident in C_2C_{12} MPD constructs with reduced differentiation phenotypes. Also as parental 'older' C_2 cells in monolayer display increased IGFBP2 expression and reduced regeneration vs. their 'younger' daughter C_2C_{12} cells that display decreased IGFBP2 expression over time (Sharples *et al.*, 2010).

Tumour necrosis factor-alpha (TNF-α) is a pleiotropic cytokine implicated as a mediator of muscle wasting in many disease states and in ageing (Leger *et al.*, 2008). TNF-α is increased significantly at 7 days in the MPD constructs vs. CON, at a time, when CON cells seem to be fusing and MPD are perhaps still proliferating. Interestingly, it has previously been shown that TNF-α is required for early satellite cell activation following damage and inflammation. However, TNF-α if chronically elevated can lead to muscle wasting (Stewart *et al.*, 2004), suggesting that in MPD constructs, the elevation in TNF may sustain proliferation at the expense of differentiation in these constructs. Further, myostatin a negative regulator of skeletal muscle mass (McPherron & Lee, 1997) that reportedly blocks differentiation of myoblasts into myotubes by reducing myoD, myogenin and protein synthetic pathways via Akt in C_2C_{12} myotubes (McFarlane *et al.*, 2006) and human skeletal myoblasts (Trendelenburg *et al.*, 2009) mirrors the profile of expression of TNF and is also increased at 7 days. Therefore, may be involved in the lack of differentiation observed. However, the data suggesting a link between myostatin and the degeneration of skeletal muscle with ageing are controversial, with some evidence for a contributing role (Leger *et al.*, 2008) and some refuting this role (Ratkevicius *et al.*, 2011) and thus requires further investigation especially because of its potential therapeutic role in reversing other muscle wasting conditions in rodents (Whittemore *et al.*, 2003).

Finally, the MPD cells once seeded into the collagen matrices showed reduced peak force measured over the first 24 h after seeding and reduced bowing. This was also accompanied with an early inability to produce MMPs 2 and 9, which have previously been implicated in muscle cellular ability to remodel the extracellular environment to migrate and differentiate (Lewis *et al.*, 2000; Morgan *et al.*, 2010). This would

suggest that the MPD cells cannot adequately remodel the matrix to align and fuse as efficiently as the parental control cells. With ageing, especially following damage it could be hypothesized that the ability of the cells to attach and remodel the matrix may contribute to the inability to regenerate and may even precede and thus hamper fusion capacity. Therefore, muscle ageing requires closer examination with regard to MMPs and even integrin and vinclulin changes in this model, in both muscle cells isolated from elderly individuals and from whole tissue, as there is a distinct lack of investigation. Especially in light of evidence suggesting relaxin overexpression can increase MMP activity and regeneration in old mice (Mu *et al.*, 2010). Elderly individuals also display reduced rate of force development (Degens *et al.*, 2009) and force per cross sectional area of muscle (Morse *et al.*, 2005b) potentially owing to the muscles efficiency of force transfer through the extracellular matrix, that maybe influenced by levels of MMP's.

Conclusion

In vitro three-dimensional (3D) bioengineered collagen constructs that incorporate multiple population doubled myoblasts under uniaxial tension, display myotube hampered hypertrophy vs. their parental control cells. Thus, by using 3D bioengineered collagen constructs these cells can be used to create an aligned myotube system that has morphologically atrophied myotubes to parental constructs, modelling aged/atrophied skeletal muscle *in-vivo.* These constructs also display reduced peak force development upon attachment, and reduced construct bowing, reduced matrix remodelling potential (reduced MMP2 and MMP9 mRNA expression), with reduced hypertrophic potential (reduced myogenin, IGF-I, IGF-IR, IGF-IEa, MGF and increased IGFBP2 mRNA) and finally increased expression of catabolic transcripts (myostatin and TNF-α). All of which have been shown to be altered during degeneration of skeletal muscle with age measured in both isolated muscle derived cells or tissue from muscle biopsies. This *in vitro* bioengineered model therefore provides an aged/atrophied system that can be experimentally manipulated by pharmacological, gene and 'exercise' therapies (mechanical stretch and electrical stimulation) to further investigate the cellular and molecular mechanisms for reduced regeneration observed with ageing in conjunction with therapeutic interventions.

Conflicts of interest

There are no conflicts of interest for the authors to declare.

References

Al-Shanti N, Stewart CE (2008) PD98059 enhances C2 myoblast differentiation through p38 MAPK activation: a novel role for PD98059. *J. Endocrinol.* **198**, 243–252.

Barton-Davis ER, Shoturma DI, Musaro A, Rosenthal N, Sweeney HL (1998) Viral mediated expression of insulin-like growth factor I blocks the aging-related loss of skeletal muscle function. *Proc. Natl. Acad. Sci. U S A* **95**, 15603–15607.

Beccafico S, Riuzzi F, Puglielli C, Mancinelli R, Fulle S, Sorci G, Donato R (2010) Human muscle satellite cells show age-related differential expression of S100B protein and RAGE. *Age (Dordr)* **33**, 523–541.

Benbassat CA, Maki KC, Unterman TG (1997) Circulating levels of insulin-like growth factor (IGF) binding protein-1 and -3 in aging men: relationships to insulin, glucose, IGF, and dehydroepiandrosterone sulfate levels and anthropometric measures. *J. Clin. Endocrinol. Metab.* **82**, 1484–1491.

Berkes CA, Tapscott SJ (2005) MyoD and the transcriptional control of myogenesis. *Semin. Cell Dev. Biol.* **16**, 585–595.

Bigot A, Jacquemin V, Debacq-Chainiaux F, Butler-Browne GS, Toussaint O, Furling D, Mouly V (2008) Replicative aging down-regulates the myogenic regulatory factors in human myoblasts. *Biol. Cell* **100**, 189–199.

Binkert C, Landwehr J, Mary JL, Schwander J, Heinrich G (1989) Cloning, sequence analysis and expression of a cDNA encoding a novel insulin-like growth factor binding protein (IGFBP-2). *EMBO J.* **8**, 2497–2502.

Blau HM, Pavlath GK, Hardeman EC, Chiu CP, Silberstein L, Webster SG, Miller SC, Webster C (1985) Plasticity of the differentiated state. *Science* **230**, 758–766.

Cheema U, Yang SY, Mudera V, Goldspink GG, Brown RA (2003) 3-D in vitro model of early skeletal muscle development. *Cell Motil Cytoskeleton* **54**, 226–236.

Cheema U, Brown R, Mudera V, Yang SY, McGrouther G, Goldspink G (2005) Mechanical signals and IGF-I gene splicing in vitro in relation to development of skeletal muscle. *J. Cell. Physiol.* **202**, 67–75.

Coolican SA, Samuel DS, Ewton DZ, McWade FJ, Florini JR (1997) The mitogenic and myogenic actions of insulin-like growth factors utilize distinct signaling pathways. *J. Biol. Chem.* **272**, 6653–6662.

Cruz-Jentoft AJ, Landi F, Topinkova E, Michel JP (2010) Understanding sarcopenia as a geriatric syndrome. *Curr. Opin. Clin. Nutr. Metab. Care.* **13**, 1–7.

Cuthbertson D, Smith K, Babraj J, Leese G, Waddell T, Atherton P, Wackerhage H, Taylor PM, Rennie MJ (2005) Anabolic signaling deficits underlie amino acid resistance of wasting, aging muscle. *Faseb J* **19**, 422–424.

Degens H, Erskine R, Morse CI (2009) Disproportionate changes in skeletal muscle strength and size with resistance training and ageing **9**, pp. 123–129.

Eastwood M, McGrouther DA, Brown RA (1994) A culture force monitor for measurement of contraction forces generated in human dermal fibroblast cultures: evidence for cell-matrix mechanical signalling. *Biochim. Biophys. Acta* **1201**, 186–192.

Edstrom E, Ulfhake B (2005) Sarcopenia is not due to lack of regenerative drive in senescent skeletal muscle. *Aging Cell* **4**, 65–77.

Ernst CW, McCusker RH, White ME (1992) Gene expression and secretion of insulin-like growth factor-binding proteins during myoblast differentiation. *Endocrinology* **130**, 607–615.

Ferri P, Barbieri E, Burattini S, Guescini M, D'Emilio A, Biagiotti L, Del Grande P, De Luca A, Stocchi V, Falcieri E (2009) Expression and subcellular localization of myogenic regulatory factors during the differentiation of skeletal muscle C2C12 myoblasts. *J. Cell. Biochem.* **108**, 1302–1317.

Florini JR, Ewton DZ, Coolican SA (1996) Growth hormone and the insulin-like growth factor system in myogenesis. *Endocr. Rev.* **17**, 481–517.

Gillies AR, Lieber RL (2011) Structure and function of the skeletal muscle extracellular matrix. *Muscle Nerve* **44**, 318–331.

Hameed M, Orrell RW, Cobbold M, Goldspink G, Harridge SD (2003) Expression of IGF-I splice variants in young and old human skeletal muscle after high resistance exercise. *J. Physiol.* **547**, 247–254.

Hameed M, Lange KH, Andersen JL, Schjerling P, Kjaer M, Harridge SD, Goldspink G (2004) The effect of recombinant human growth hormone and resistance training on IGF-I mRNA expression in the muscles of elderly men. *J. Physiol.* **555**, 231–240.

Heron-Milhavet L, Mamaeva D, LeRoith D, Lamb NJ, Fernandez A (2010) Impaired muscle regeneration and myoblast differentiation in mice with a muscle-specific KO of IGF-IR. *J. Cell. Physiol.* **225**, 1–6.

Hidestrand M, Richards-Malcolm S, Gurley CM, Nolen G, Grimes B, Waterstrat A, Zant GV, Peterson CA (2008) Sca-1-expressing nonmyogenic cells contribute to fibrosis in aged skeletal muscle. *J. Gerontol. A Biol. Sci. Med. Sci.* **63**, 566–579.

Hughes VA, Frontera WR, Wood M, Evans WJ, Dallal GE, Roubenoff R, Fiatarone Singh MA (2001) Longitudinal muscle strength changes in older adults: influence of muscle mass, physical activity, and health. *J. Gerontol. Series A Biol. Sci. Med. Sci.* **56**, B209–B217.

Jacquemin V, Furling D, Bigot A, Butler-Browne GS, Mouly V (2004) IGF-1 induces human myotube hypertrophy by increasing cell recruitment. *Exp. Cell Res.* **299**, 148–158.

Leger B, Derave W, De Bock K, Hespel P, Russell AP (2008) Human sarcopenia reveals an increase in SOCS-3 and myostatin and a reduced efficiency of Akt phosphorylation. *Rejuvenation Res.* **11**, 163–175B.

Lewis MP, Tippett HL, Sinanan AC, Morgan MJ, Hunt NP (2000) Gelatinase-B (matrix metalloproteinase-9; MMP-9) secretion is involved in the migratory phase of human and murine muscle cell cultures. *J. Muscle Res. Cell Motil.* **21**, 223–233.

Mauro A (1961) Satellite cell of skeletal muscle fibers. *J. Biophys. Biochem. Cytol.* **9**, 493–495.

McFarlane C, Plummer E, Thomas M, Hennebry A, Ashby M, Ling N, Smith H, Sharma M, Kambadur R (2006) Myostatin induces cachexia by activating the ubiquitin proteolytic system through an NF-kappaB-independent, FoxO1-dependent mechanism. *J. Cell. Physiol.* **209**, 501–514.

McPherron AC, Lee SJ (1997) Double muscling in cattle due to mutations in the myostatin gene. *Proc. Natl. Acad. Sci. U S A* **94**, 12457–12461.

Miyazaki M, McCarthy JJ, Fedele MJ, Esser KA (2011) Early activation of mTORC1 signalling in response to mechanical overload is independent of phosphoinositide 3-kinase/Akt signalling. *J. Physiol.* **589**, 1831–1846.

Morgan J, Rouche A, Bausero P, Houssaini A, Gross J, Fiszman MY, Alameddine HS (2010) MMP-9 overexpression improves myogenic cell migration and engraftment. *Muscle Nerve* **42**, 584–595.

Morse CI, Thom JM, Birch KM, Narici MV (2005a) Changes in triceps surae muscle architecture with sarcopenia. *Acta Physiol. Scand.* **183**, 291–298.

Morse CI, Thom JM, Reeves ND, Birch KM, Narici MV (2005b) In vivo physiological cross-sectional area and specific force are reduced in the gastrocnemius of elderly men. *J. Appl. Physiol.* **99**, 1050–1055.

Mouly V, Aamiri A, Bigot A, Cooper RN, Di Donna S, Furling D, Gidaro T, Jacquemin V, Mamchaoui K, Negroni E, Perie S, Renault V, Silva-Barbosa SD, Butler-Browne GS (2005) The mitotic clock in skeletal muscle regeneration, disease and cell mediated gene therapy. *Acta Physiol. Scand.* **184**, 3–15.

Mu X, Urso ML, Murray K, Fu F, Li Y (2010) Relaxin regulates MMP expression and promotes satellite cell mobilization during muscle healing in both young and aged mice. *Am. J. Pathol.* **177**, 2399–2410.

Mudera V, Smith AS, Brady MA, Lewis MP (2010) The effect of cell density on the maturation and contractile ability of muscle derived cells in a 3D tissue-engineered skeletal muscle model and determination of the cellular and mechanical stimuli required for the synthesis of a postural phenotype. *J. Cell. Physiol.* **225**, 646–653.

O'Connor MS, Carlson ME, Conboy IM (2009) Differentiation rather than aging of muscle stem cells abolishes their telomerase activity. *Biotechnol. Prog.* **25**, 1130–1137.

Owino V, Yang SY, Goldspink G (2001) Age-related loss of skeletal muscle function and the inability to express the autocrine form of insulin-like growth factor-1 (MGF) in response to mechanical overload. *FEBS Lett.* **505**, 259–263.

Pietrangelo T, Puglielli C, Mancinelli R, Beccafico S, Fano G, Fulle S (2009) Molecular basis of the myogenic profile of aged human skeletal muscle satellite cells during differentiation. *Exp. Gerontol.* **44**, 523–531.

Player DJ, Martin NRW, Castle PC, Sharples AP, Passey S, Mudera V, Lewis MP (2011) A putative model of endurance exercise using bio-engineered skeletal muscle. *Proc. Physiol. Soc.* **23**, PC333.

Quinn LS, Anderson BG, Plymate SR (2007) Muscle-specific overexpression of the type 1 IGF receptor results in myoblast-independent muscle hypertrophy via PI3K, and not calcineurin, signaling. *Am. J. Physiol. Endocrinol. Metab.* **293**, E1538–E1551.

Rantanen T, Harris T, Leveille SG, Visser M, Foley D, Masaki K, Guralnik JM (2000) Muscle strength and body mass index as long-term predictors of mortality in initially healthy men. *J. Gerontol. A Biol. Sci. Med. Sci.* **55**, M168–73.

Ratkevicius A, Joyson A, Selmer I, Dhanani T, Grierson C, Tommasi AM, DeVries A, Rauchhaus P, Crowther D, Alesci S, Yaworsky P, Gilbert F, Redpath TW, Brady J, Fearon KC, Reid DM, Greig CA, Wackerhage H (2011) Serum concentrations of myostatin and myostatin-interacting proteins do not differ between young and sarcopenic elderly men. *J. Gerontol. A Biol. Sci. Med. Sci.* **66**, 620–626.

Rosenberg IH (1997) Sarcopenia: origins and clinical relevance. *J. Nutr.* **127** (5 Suppl), 990S–991S.

Russ DW, Lanza IR (2011) The impact of old age on skeletal muscle energetics: supply and demand. *Curr. Aging Sci.* **4**, 234–247.

Schmittgen TD, Livak KJ (2008) Analyzing real-time PCR data by the comparative C(T) method. *Nat. Protoc.* **3**, 1101–1108.

Sharples AP, Stewart CE (2011) Myoblast models of skeletal muscle hypertrophy and atrophy. *Curr. Opin. Clin. Nutr. Metab. Care* **14**, 230–236.

Sharples AP, Al-Shanti N, Stewart CE (2010) C2 and C2C12 murine skeletal myoblast models of atrophic and hypertrophic potential: relevance to disease and ageing? *J. Cell. Physiol.* **225**, 240–250.

Sharples AP, Al-Shanti N, Lewis MP, Stewart CE (2011) Reduction of myoblast differentiation following multiple population doublings in mouse C(2) C(12) cells: a model to investigate ageing? *J. Cell. Biochem.* **112**, 3773–3785.

Smith AS, Passey S, Greensmith L, Mudera V, Lewis MP (2011) Characterisation and optimisation of a simple, repeatable system for the long term in vitro culture of aligned myotubes in 3D. *J. Cell. Biochem.* **113**, 1044–1053.

Spangenburg EE, Le Roith D, Ward CW, Bodine SC (2008) A functional insulin-like growth factor receptor is not necessary for load-induced skeletal muscle hypertrophy. *J. Physiol.* **586**, 283–291.

Stewart CE, Rotwein P (1996) Growth, differentiation, and survival: multiple physiological functions for insulin-like growth factors. *Physiol. Rev.* **76**, 1005–1026.

Stewart CE, Newcomb PV, Holly JM (2004) Multifaceted roles of TNF-alpha in myoblast destruction: a multitude of signal transduction pathways. *J. Cell. Physiol.* **198**, 237–247.

Trendelenburg AU, Meyer A, Rohner D, Boyle J, Hatakeyama S, Glass DJ (2009) Myostatin reduces Akt/TORC1/p70S6K signaling, inhibiting myoblast differentiation and myotube size. *Am. J. Physiol. Cell Physiol.* **296**, C1258–C1270.

Welle S, Bhatt K, Shah B, Thornton C (2002) Insulin-like growth factor-1 and myostatin mRNA expression in muscle: comparison between 62-77 and 21-31 yr old men. *Exp. Gerontol.* **37**, 833–839.

Wheatcroft SB, Kearney MT (2009) IGF-dependent and IGF-independent actions of IGF-binding protein-1 and -2: implications for metabolic homeostasis. *Trends Endocrinol. Metab.* **20**, 153–162.

Whittemore LA, Song K, Li X, Aghajanian J, Davies M, Girgenrath S, Hill JJ, Jalenak M, Kelley P, Knight A, Maylor R, O'Hara D, Pearson A, Quazi A, Ryerson S, Tan XY, Tomkinson KN, Veldman GM, Widom A, Wright JF, Wudyka S, Zhao L, Wolfman NM (2003) Inhibition of myostatin in adult mice increases skeletal muscle mass and strength. *Biochem. Biophys. Res. Commun.* **300**, 965–971.

Yaffe D, Saxel O (1977) Serial passaging and differentiation of myogenic cells isolated from dystrophic mouse muscle. *Nature* **270**, 725–727.

Yang SY, Goldspink G (2002) Different roles of the IGF-I Ec peptide (MGF) and mature IGF-I in myoblast proliferation and differentiation. *FEBS Lett.* **522**, 156–160.